All-solid-state synchronously pumped optical parametric oscillator

M. J. McCarthy and D. C. Hanna

Optoelectronics Research Centre, University of Southampton, Southampton SO9 5NH, UK

Received November 4, 1992; revised manuscript received April 7, 1993

The design and performance of a continuously operated singly resonant synchronously pumped potassium titanyl phosphate optical parametric oscillator is described. With an all-solid-state pump source providing 2-ps pulses at 523 nm, we found that the oscillation threshold pump intensity was ~60 MW cm^{-2}, in good agreement with design calculations. The output of the optical parametric oscillator provided transform-limited pulses of 1–2-ps duration at a 125-MHz repetition rate, continuously tunable over the range of 938–1184 nm, with tens of milliwatts of average power.

1. INTRODUCTION

The initial demonstration of the optical parametric oscillator (OPO) by Giordmaine and Miller in 1965 (Ref. 1) generated a great deal of interest, since these devices were seen to offer a means to wide tunability of coherent light sources. Development of OPO's was hampered in the early days by the problem of optical damage to the nonlinear crystal. Also, OPO's typically have broad gain bandwidths, together with the broad tuning range, so that an additional complexity in the form of intracavity frequency-selecting devices was generally necessary. These difficulties with OPO's led to a certain amount of disenchantment after the initial excitement. On the other hand, it was realized that pumping of an OPO with ultrashort pulses offered considerable attractions. This device not only was useful, offering a broadly tunable source of ultrashort pulses and thus exploiting the broad gain bandwidth, but also had a greatly reduced damage problem, since much higher intensities could be withstood in short pump pulses rather than in *Q*-switched pulses. Synchronously pumped OPO's (SPOPO's) were subsequently demonstrated in a variety of gain media with actively mode-locked lasers pumped by flash lamps,[2-5] generally with a pulsed envelope of mode-locked pulses to achieve sufficient pump intensity.

For practical use a cw pump source is desirable, so that the output consists of identical pulses at high repetition rates (hundreds of megahertz). These features are essential to the attainment of high signal-to-noise ratio data in many spectroscopic experiments. Continuous operation of a SPOPO was demonstrated by Piskarskas *et al.*[6] They used the frequency-doubled output of an actively mode-locked Nd:YAG laser to operate a cw SPOPO in a doubly resonant oscillator (DRO) configuration, using $Ba_2NaNb_5O_{12}$ as the gain medium. Although the DRO configuration results in a comparatively low oscillation threshold, it is inherently sensitive to perturbations. The requirements for simultaneous resonance for both the generated waves place stringent stability demands on the pump laser and the OPO cavity. This generally results in poor amplitude and frequency stability and in erratic tuning behavior. This problem is exacerbated in the case of ultrashort pulse operation, in which material dispersion and birefringence of the nonlinear crystal prevent maintenance of the resonance condition across a broad comb of modes.

Resonating only one of the generated waves in a singly resonant oscillator (SRO) can greatly relax the tolerances on the pump laser and OPO cavity. However, this typically results in more than an order-of-magnitude increase in the oscillation threshold condition. The requirements of generating sufficiently high peak power for operation of a SRO, together with cw pumping, can be met through the use of ultrashort pump pulses. Edelstein *et al.*[7] and Wachman *et al.*[8,9] operated a cw SPOPO in a singly resonant configuration, using potassium titanyl phosphate (KTP) as the gain medium and a colliding-pulse mode-locked dye laser as the pump source. They achieved transform-limited pulses of ~100-fs duration tunable over the range of 760–1040 nm and pulses of ~200-fs duration tunable over the range of 1500–3200 nm, with average powers of a few milliwatts. This was the first demonstration of a cw singly resonant SPOPO and also the first demonstration of a SPOPO in the femtosecond domain. However, the limited average power available from the dye laser necessitated the complicating feature of the SPOPO's being sited at an intracavity focus to permit access to sufficiently high peak intensities. The conversion efficiency of this device was limited to ~10%. Mak *et al.*[10] demonstrated cw operation of an externally pumped femtosecond SRO, using KTP as the gain medium and a synchronously mode-locked dye laser as the pump source. Pulses of 220-fs duration tunable from 1200–1340 nm were demonstrated with tens of milliwatts of average power. More recently, KTP SPOPO's have been demonstrated with Kerr-lens mode-locked Ti:sapphire lasers as the pump lasers.[11,12] These have generated pulses of ~100-fs duration tunable over the ranges of 1200–1400 and 1800–2200 nm, with hundreds of milliwatts of average power.

An important step in the development of a practical system must be the move to laser diodes as the basic source of pump power. Steps in this direction include the use by

0740-3224/93/112180-11$06.00 © 1993 Optical Society of America

Maker and Ferguson[13] of a frequency-doubled Q-switched and mode-locked diode-pumped Nd:YAG laser to achieve oscillation in a SPOPO based on $MgO:LiNbO_3$. They achieved picosecond pulses tunable over the range of 983–1119 nm but with very poor stability because of the doubly resonant nature of the device. Similar pulsed pumped systems with KTP or lithium triborate (LBO) as the gain medium were demonstrated by Ebrahimzadeh *et al.*[14,15] The KTP oscillator provided angle tuning over the ranges of 946–1020 and 1075–1172 nm,[14] whereas the LBO oscillator could be temperature tuned over the range of 650–2700 nm.[15] Ebrahimzadeh *et al.*[16] also demonstrated cw synchronous pumping of a KTP OPO, using a frequency-doubled actively mode-locked laser as the pump source. This device was again doubly resonant and therefore suffered from poor amplitude stability. By pumping with shorter pump pulses we were able to demonstrate SRO operation of a KTP SPOPO with the excellent amplitude stability that is the hallmark of singly resonant operation.[17] More recently, Robertson *et al.*[18] have reported cw synchronous pumping of a singly resonant LBO device, with a tuning range of 0.65–2.7 μm.

In this paper we present detailed results for our singly resonant SPOPO with KTP as the gain medium. The pump source for this system is a frequency-doubled self-starting additive-pulse mode-locked Nd:YLF laser pumped by a 3-W laser diode. An important feature of this laser is that it produced much shorter pulses and hence higher peak powers than an actively mode-locked system and thus enabled singly resonant oscillation to be easily achieved. In Section 2 we develop quantitative estimates of the gain and hence threshold of the SPOPO, taking into account the three-dimensional confinement of the interacting fields and the finite acceptance parameters of the nonlinear crystal. In Section 3 we present pertinent parameters for two nonlinear materials, KTP and LBO. The suitability of each for operation in a singly resonant SPOPO with a laser-diode pump source is considered. In Section 4 we describe the experimental arrangement and present results for a SRO with KTP as the gain medium. A concluding discussion in Section 5 draws together these results with the calculations for LBO to point out possible future developments for the laser-diode-pumped SPOPO.

2. PARAMETRIC-GAIN CALCULATION

Treatments that address the situation of confined fields within a parametric interaction have been provided by a number of authors. Boyd and Kleinman[19] treated the problem of stationary second-harmonic generation and parametric generation (DRO) with focused Gaussian beams, including in their analysis the effects of diffraction of the beams within the nonlinear crystal. Guha and Falk[20] extended this approach to the case of the SRO.[20] More recently, Cheung and Liu[21,22] have made detailed numerical investigations of SPOPO performance. They allowed for spatial confinement and diffraction and temporal confinement of the interacting fields. In all these investigations the researchers used computer techniques to solve the relevant equations numerically. In making the design choices for the SPOPO that we demonstrate here, we recognized the need to have available a simple analytical model that, although approximate, at least gives quantitative guidelines that can be readily applied to any SPOPO. This model must show in a transparent way the effect on parametric gain of such dominant parameters as crystal length, group-velocity dispersion, double-refraction walk-off, spectral acceptance, and angular acceptance. In developing this model we build on the research of Brosnan and Byer[23] and of Edelstein.[24] The main concern of the designer is to ensure that threshold can be reached, so the model presented here is intended only to calculate the small-signal gain of the SPOPO and thus to predict the oscillation threshold condition. We make no attempt to account for the effects of pump depletion. In any case there is the comforting observation that, once above threshold, OPO's typically have rather high conversion efficiencies. Additionally, we make no attempt to describe the temporal characteristics of the output radiation. An analytical model describing the temporal output of a SPOPO was previously presented by Becker *et al.*[25]

The parametric growth of the signal- and idler-field amplitudes E_s, E_i at frequencies ω_s, ω_i in a nonlinear crystal in the presence of a pump-field amplitude E_p at frequency ω_p is described by a pair of coupled differential equations. For collinear plane waves propagating along the z axis in the slowly varying envelope approximation and assuming no pump depletion, they are[26]

$$\frac{dE_s}{dz} = j\kappa_s E_p E_i^* \exp(j\Delta k z), \tag{1}$$

$$\frac{dE_i}{dz} = j\kappa_i E_p E_s^* \exp(j\Delta k z). \tag{2}$$

Here $\Delta k = k_p - (k_s + k_i)$ is the wave-vector mismatch. The interaction coefficients κ_m $(m = s, i)$ are given by

$$\kappa_m = \frac{\omega_m d_{\text{eff}}}{n_m c}. \tag{3}$$

In Eq. (3), d_{eff} is the effective nonlinear coefficient, n_m is the refractive index of the nonlinear crystal at the frequency ω_m, and c is the speed of light in free space. Solving Eqs. (1) and (2) yields expressions for the signal- and idler-field amplitudes after propagation through a gain interaction length l_g. For a phase-matched interaction $\Delta k = 0$ they are[26]

$$E_s(l_g) = E_s(0)\cosh(\Gamma l_g) + j\frac{\kappa_s E_p}{\Gamma} E_i^*(0)\sinh(\Gamma l_g), \tag{4}$$

$$E_i(l_g) = E_i(0)\cosh(\Gamma l_g) + j\frac{\kappa_s E_p}{\Gamma} E_s^*(0)\sinh(\Gamma l_g). \tag{5}$$

The parametric amplitude gain coefficient Γ is given by

$$\Gamma = (\kappa_s \kappa_i |E_p|^2)^{1/2}. \tag{6}$$

One determines the oscillation threshold condition for an OPO by requiring that the round-trip loss experienced by the resonated wave(s) be exactly balanced by the gain. For a SRO the idler wave is not resonated, and the return field to the gain medium is $E_i(0) = 0$. The oscillation threshold condition for the signal wave is

$$E_s(0) = (1 - \alpha_s) E_s(l_g), \tag{7}$$

where α_s is the round-trip amplitude attentuation for the resonated signal wave. Substituting for $E_s(l_g)$ from Eq. (4), one can write Eq. (7) as

$$(1 - \alpha_s)\cosh(\Gamma l_g) = 1. \tag{8}$$

In the approximation of small loss ($\Gamma l_g, \alpha_s \ll 1$) the oscillation threshold condition for the SRO becomes[26]

$$\Gamma^2 l_g^2 = 2\alpha_s = L, \tag{9}$$

where L is the round-trip intensity loss for the resonated signal wave.

Practical SPOPO's almost invariably involve the pump-laser beams' having a TEM_{00} Gaussian spatial profile and the resonated signal beams' also having a Gaussian spatial profile. Brosnan and Byer[23] extended the plane-wave model of optical parametric amplification to include the feature of Gaussian beams. Their near-field analysis accounted for the transverse dependence of the signal, idler, and pump fields but assumed that this dependence did not change over the length of the nonlinear crystal, i.e., diffraction of the beams was neglected. For this approximation to be valid, one requires that the confocal parameters of all three beams be at least as long as the nonlinear crystal. Brosnan and Byer also allowed for Poynting-vector walk-off of the pump field from the signal and idler fields, as exhibited by the type-I parametric interaction in $LiNbO_3$ that they were modeling. In the SPOPO, by virtue of the short temporal and hence spatial extent of the light pulses, the pump, signal, and idler fields are confined in the direction of propagation as well as in the transverse plane. Thus, in addition to progressive spatial separation of the fields in the plane transverse to the direction of propagation that is due to Poynting-vector walk-off, there will also be separation of the fields in the direction of propagation because of group-velocity mismatch among the various pulse envelopes. The Brosnan–Byer theory is easily extended to include confinement in three dimensions. In addition, one can introduce separate Poynting-vector walk-off angles for the three interacting fields to describe a type-II interaction. Group-velocity walk-off among the pump, the signal, and the idler pulse envelopes can be described through the space–time analogy of Akhmanov *et al.*[27] The description here neglects dispersive broadening of the pulses, which was negligible for the conditions of our experiments with pulses of ~1-ps duration but becomes a consideration for pulses in the femtosecond regime. Nonlinear effects such as self-phase modulation of the intense pump and signal beams in the nonlinear medium are also not considered.

The signal field has a Gaussian transverse dependence of the form

$$E_s r = E_{s0} \exp - \left(\frac{r^2}{w_s^2}\right). \tag{10}$$

Here w_s is the signal-field beam radius or spot size ($1/e$ amplitude). Similar expressions describe the pump and idler fields. The driving polarization at the signal frequency is generated by mixing of the pump and idler fields, i.e., $P_s = 2\epsilon_0 d_{\text{eff}} E_i^* E_p$. Then the spatial profile of the signal polarization wave also has a Gaussian transverse dependence, with a beam radius $\overline{w}_s$ given by

$$\frac{1}{\overline{w}_s^2} = \frac{1}{w_i^2} + \frac{1}{w_p^2}. \tag{11}$$

A similar equation exists for the beam radius $\overline{w}_i$ of the idler polarization wave, i.e.,

$$\frac{1}{\overline{w}_i^2} = \frac{1}{w_s^2} + \frac{1}{w_p^2}. \tag{12}$$

In the SRO the idler field is nonresonant and is presumed to assume a waist size so as to maximize coupling to the idler polarization, i.e.,

$$\overline{w}_i = w_i. \tag{13}$$

In the direction of propagation, one assumes that the pump and signal fields, for analytical convenience, have Gaussian envelopes. Thus one can write expressions that are similar to Eqs. (10)–(13) for the time dependence of the envelopes in terms of τ_m ($m = p, s, i$) where $2\tau_m$ is the field $1/e$ amplitude pulse width.

In deriving the parametric gain for the signal field, one must consider only that portion of the generated signal wave that couples into the TEM_{00} mode of the resonator. This is conveniently described by the coupling coefficient formalism of Kogelnik.[28] The coupling coefficient c_s between the signal polarization wave and the resonated signal field is given by

$$c_s = \int_{-\infty}^{+\infty} P_s(x)E_s(x)\mathrm{d}x \int_{-\infty}^{+\infty} P_s(y)E_s(y)\mathrm{d}y \int_{-\infty}^{+\infty} P_s(t)E_s(t)\mathrm{d}t, \tag{14}$$

where $E_s(x)$, $E_s(y)$, and $E_s(t)$ are normalized.

Considering the case of phase matching within a principal plane of the nonlinear crystal, we define Poynting-vector walk-off as confined to the coordinate plane $y = 0$. For type-II phase matching in the crystallographic xy plane in KTP the pump and signal fields are extraordinary waves and the idler field is an ordinary wave. This serves as a convenient choice of reference frame to describe the relative propagation of the three beams. The choice of coordinate frame in the direction of propagation is somewhat arbitrary, and the propagation of the signal and idler pulses is described relative to the propagation of the pump pulse. According to the analyses of Brosnan and Byer[23] and Edelstein,[24] the signal coupling coefficient c_s is thus explicitly given from Eq. (14) by

$$\begin{aligned} c_s = {} & [2/(\pi w_s^2)]^{1/2} \int_{-\infty}^{+\infty} \mathrm{d}x \\ & \times \exp - \left[\frac{(x - \rho_s z)^2}{w_s^2} + \frac{x^2}{w_i^2} + \frac{(x - \rho_p z)^2}{w_p^2}\right] \\ & \times [2/(\pi w_s^2)]^{1/2} \int_{-\infty}^{+\infty} \mathrm{d}y \exp - \left[\frac{y^2}{w_s^2} + \frac{y^2}{w_i^2} + \frac{y^2}{w_p^2}\right] \\ & \times [2/(\pi \tau_s^2)]^{1/2} \int_{-\infty}^{+\infty} \mathrm{d}t \\ & \times \exp - \left[\frac{(t - \nu_s z)^2}{\tau_s^2} + \frac{(t - \nu_i z)^2}{\tau_i^2} + \frac{t^2}{\tau_p^2}\right]. \end{aligned} \tag{15}$$

Here $\rho_{s(p)}$ is the signal- (pump-) field Poynting-vector walk-off angle that one calculates by using the appropriate Sellmeier equations. $\nu_{s(i)}$ is the group-velocity walk-off of

the signal (idler) pulse relative to the pump pulse, i.e.,

$$v_{s(i)} = \frac{1}{v_{gs(i)}} - \frac{1}{v_{gp}}, \tag{16}$$

where $v_{gs(i,p)}$ is the group velocity of the signal (idler, pump) field in the nonlinear crystal. Again, one calculates these by using the appropriate Sellmeier equations. Performing the integration in Eq. (15), one obtains

$$c_s = g_s g_t \exp\left(-\frac{\pi}{4}\frac{z^2}{l_w^2}\right), \tag{17}$$

where

$$g_s = \frac{w_p^2}{w_s^2 + w_p^2}, \tag{18}$$

$$g_t = [\tau_p^2/(\tau_s^2 + \tau_p^2)]^{1/2}. \tag{19}$$

The aperture length l_w is given by

$$\frac{1}{l_w^2} = \frac{1}{l_s^2} + \frac{1}{l_t^2}, \tag{20}$$

where the spatial aperture length l_s is given by

$$l_s = \frac{\sqrt{\pi}}{2}\left(\left(\frac{\rho_s^2}{w_s^2} + \frac{\rho_p^2}{w_p^2}\right) - \left\{\frac{[(\rho_s/w_s^2) + (\rho_p/w_p^2)]^2}{2[(1/w_s^2) + (1 + w_p^2)]}\right\}\right)^{-1/2} \tag{21}$$

and the temporal aperture length l_t is given by

$$l_t = \frac{\sqrt{\pi}}{2}\left(\left[\frac{\nu_s^2}{\tau_s^2} + \nu_i^2\left(\frac{1}{\tau_s^2} + \frac{1}{\tau_p^2}\right)\right] - \frac{\{(\nu_s/\tau_s^2) + \nu_i[(1/\tau_s^2) + (1/\tau_p^2)]\}^2}{2[(1/\tau_s^2) + (1/\tau_p^2)]}\right)^{-1/2}. \tag{22}$$

The corresponding result for the idler gives the idler coupling coefficient c_i as

$$c_i = \exp\left(-\frac{\pi}{4}\frac{z^2}{l_w^2}\right). \tag{23}$$

Incorporation of these coupling coefficients into the coupled parametric-gain Eqs. (1) and (2) leads to modified expressions for the parametric-gain coefficient and the interaction length in Eqs. (4) and (5). One defines the modified parametric-gain coefficient Γ' as

$$\Gamma' = \left(\frac{2\omega_s\omega_i d_{\text{eff}}^2}{n_s n_i n_p \epsilon_0 c^3} g_s g_t I_p\right)^{1/2}, \tag{24}$$

where the pump intensity I_p has been substituted for E_p according to

$$I_p = \tfrac{1}{2} n_p c \epsilon_0 |E_p|^2. \tag{25}$$

Here ϵ_0 is the permittivity of free space. For a SPOPO it is the peak intensity that determines the parametric gain. The modified gain interaction length l_g' is defined as

$$l_g' = \int_0^{l_c} \exp\left(-\frac{\pi}{4}\frac{z''^2}{l_w^2}\right) dz'' \tag{26}$$

$$= l_w \operatorname{erf}\left(\frac{\sqrt{\pi}}{2}\frac{l_c}{l_w}\right), \tag{27}$$

where l_c is the length of the nonlinear crystal. For large arguments the error function approaches unity, and l_w is the effective gain length. The spatial part of l_w, l_s [Eq. (21)] describes the reduction in the interaction length resulting from Poynting-vector spatial separation of the interacting fields. The temporal part, l_t [Eq. (22)], describes the reduction of the interaction length resulting from group-velocity temporal separation of the pulse envelopes.

One can estimate the effects of the phase-matching bandwidth and the angular-acceptance width of the nonlinear crystal on the parametric gain. For a SPOPO operating near degeneracy, one can gauge these effects by drawing on analogous results from second-harmonic generation. The reduction in parametric gain that results from use of a pump of bandwidth $\Delta\nu_p$ over that for a pump of negligible bandwidth is given by[29]

$$\frac{\eta(\Delta\nu_p)}{\eta(0)} = \frac{\int_{-\infty}^{\infty} g(\Delta\nu_p) h(\Delta\nu) d\nu}{\int_{-\infty}^{\infty} g(\Delta\nu_p) d\nu}. \tag{28}$$

Here $g(\Delta\nu_p)$ is the intensity spectral line-shape function of the pump pulses with FWHM $\Delta\nu_p$ and $h(\Delta\nu)$ is the sinc^2 function for a crystal with spectral-acceptance bandwidth FWHM of $\Delta\nu$. If the line-shape function and the sinc^2 function are approximated by Gaussians, the reduction in parametric gain is

$$\frac{\eta(\nu_p)}{\eta(0)} \simeq [\Delta\nu^2/(\Delta\nu^2 + \Delta\nu_p^2)]^{1/2}. \tag{29}$$

Expressions for the spectral-acceptance bandwidth of a nonlinear crystal have been presented in the literature, e.g., Ref. 29, and can be calculated with the appropriate Sellmeier equations.

The crystal acceptance angle will result in a similar reduction in the parametric gain because of the finite divergence of the pump beam. If one uses the same approach as for Eqs. (30) and (31), the reduction in parametric gain from a collimated-beam interaction is given by

$$\frac{\eta(\Delta\theta_p)}{\eta(0)} \simeq [\Delta\theta^2/(\Delta\theta^2 + \Delta\theta_p^2)]^{1/2}. \tag{30}$$

Here $\Delta\theta$ is the FWHM intensity-acceptance angle of the crystal, expressions for which have been presented in the literature, e.g., Refs. 30 and 31. A representative value of $\Delta\theta_p$ is considered to be one half times the FWHM intensity divergence angle of the pump beam at the entrance/exit face of the crystal. Thus

$$\Delta\theta_p = 0.4\frac{\lambda}{\pi w_0} \tag{31}$$

for a Gaussian beam that is confocally focused in the nonlinear crystal with the waist at the crystal center. The intensity parametric-gain coefficient Γ'^2 will be reduced by the factor $\eta(\Delta\theta_p)\eta(\Delta\nu_p)$.

3. NONLINEAR MEDIUM

The primary consideration in the choice of gain medium is whether sufficient gain can be achieved for oscillation.

For a nonlinear crystal to generate high parametric gain with an ultrashort-pulse pump source of modest average power, the requirements are high nonlinearity, high damage threshold, large angular acceptance, and large spectral acceptance. These attributes permit efficient conversion of a tightly focused wide-bandwidth pump beam. High optical quality and homogeneity are also paramount for low optical loss, since one will typically be dealing with low gain.

Tunability is ultimately limited by the transmission range of the material. In practice the tuning range is limited by the relative magnitudes of the birefringence and the dispersion of the principal refractive indices of the material. For angle-tuned phase-matching schemes, a large tuning range requires a large birefringence in the plane of propagation. This carries the consequence of a large Poynting-vector walk-off and small angular-acceptance width, which limits the degree of focusing. For materials with a large temperature dependence of the birefringence such that temperature-tuned noncritical phase matching can be achieved, one can accomplish tight focusing of the beams over the entire tuning range.

Below we present relevant parameters for two nonlinear crystals, KTP and LBO. Both these materials are finding applications in singly resonant SPOPO's and are currently the materials of choice.

KTP is a crystal that is characterized by large nonlinear coefficients, a high optical-damage threshold (1 GW cm^{-2} for 10-ns pulses at 1064 nm) and a wide transparency range of ~400–4500 nm.[32] Angle-tuned phase matching can be achieved over virtually this entire range. The birefringence of KTP has a small temperature dependence, making it insensitive to temperature gradients in the crystal caused by local heating, but on the other hand this does preclude the use of temperature tuning. KTP is a biaxial crystal. However, the birefringence in the xy principal plane is much smaller than in the other two principal planes, so the crystal is quasi-uniaxial. The principal indices and birefringence are such that quasi-noncritical phase matching can be achieved in the xy plane for a type-II parametric interaction between wavelengths near 1000 and 500 nm, e.g., second-harmonic generation of Nd:YAG lasers at 1064–532 nm. With this phase-matching scheme the pump wave at $\lambda_p \simeq 500$ nm is an extraordinary wave that is polarized parallel to the xy plane. The two generated waves at $\lambda_{s,i} \simeq 1000$ nm are extraordinary and ordinary waves that are polarized parallel to the xy plane and the z axis, respectively.

Whereas KTP is more dispersive than some materials, e.g., BBO and LBO, the high nonlinearity means that the spectral-acceptance bandwidth of a crystal of sufficient length to achieve high parametric gain is larger than average. The calculated spectral-acceptance-angle × length product for the degenerate interaction between 523 and 1047 nm is 0.54 nm cm at a wavelength of 1047 nm, giving a 5-mm-long crystal a spectral-acceptance bandwidth of 1.10 nm at a 1047-nm wavelength (these calculations use the dispersion relations of Bierlein and Vanherzeele[32]). The spectral bandwidth of 2-ps pulses is 0.14 nm at $\lambda_p = 523$ nm and 0.58 nm at $\lambda_{s,i} = 1047$ nm ($sech^2$ profile). Thus one calculates from relation (29) that the parametric-gain-reduction factor over a single-frequency interaction is $\eta(\Delta\nu_p) = 0.88$.

The low birefringence coupled with a type-II interaction for KTP that is phase matched in the xy plane gives a high product of length with external spatial acceptance angle. This is calculated to be 18 mrad cm in the critical direction and 61 mrad $cm^{1/2}$ in the noncritical direction. The acceptance angle of a 5-mm-long KTP crystal in this phase-matching scheme is thus 36 mrad in the critical direction and 81 mrad in the noncritical direction. One calculates from Eq. (31) that the pump-beam divergence $\Delta\theta_p$ for a 523-nm beam focused to a 16-μm waist in the KTP crystal is 4 mrad. The parametric-gain-reduction factor over a plane-wave interaction is calculated from relation (30) to be $\eta(\Delta\theta_p) = 0.99$.

One calculates that the Poynting-vector walk-off is 4.3 mrad for the signal wave that is polarized parallel to the xy plane and 6.1 mrad for the pump beam. With a signal waist size of $w_s = 20$ μm and a pump waist size of $w_p = 16$ μm, these values give a spatial aperture length of $l_s = 2.8$ mm, calculated according to Eq. (21).

The relative group delays between the pulses are calculated from Eq. (16) to be

$$\nu_{p_s} = 0.47 \text{ ps mm}^{-1}, \qquad \nu_{p_i} = 0.15 \text{ ps mm}^{-1}. \tag{32}$$

The limiting group-velocity delay is between the signal pulse and the pump pulse. The delay of 0.47 ps mm^{-1} gives a temporal pulse walk-off of 2.4 ps for a 5-mm-long crystal. For pump and signal pulses of 2.0-ps duration, one calculates from Eq. (22) that the temporal aperture length is $l_t = 4.4$ mm. From Eq. (20) the interaction length l_w is calculated to be 2.4 mm, and from Eq. (27) the parametric-gain length l' is calculated to be 2.4 mm.

With $n_p n_s n_i = 5.71$, $d_{\text{eff}} = 3.2$ pm V^{-1},[33] and a crystal length of 5 mm, one calculates the peak parametric gain by using Eqs. (24) and (27), and the calculated values of $\eta(\Delta\nu_p)$ and $\eta(\Delta\theta_p)$ are

$$\eta(\Delta\nu_p)\eta(\Delta\theta_p)\Gamma'^2 l'^2 = 7 \times 10^{-4} \text{ MW}^{-1} \text{ cm}^2. \tag{33}$$

With a pulse-repetition rate of 125 MHz and other parameters as quoted above, the parametric-gain coefficient is

$$\eta(\Delta\nu_p)\eta(\Delta\theta_p)\Gamma'^2 l'^2 = 0.7 \text{ W}^{-1}. \tag{34}$$

average power. For a cavity-round-trip loss of 3% one calculates from Eq. (9) that the threshold average pump power is 50 mW.

The primary drawback of a 523-nm-pumped SPOPO in KTP that is phase matched in the xy plane is the limited tuning range. The calculated tuning curve for a 523-nm-pumped SPOPO in KTP is shown in Fig. 1. We calculated the tuning curve by using the Sellmeier relations for KTP published by Bierlein and Vanherzeele.[32] The tuning range in the xy plane is limited to ~200 nm because of the small birefringence. Phase matching in the zx (or yz) plane, where the birefringence is larger, in principle would permit tuning across most of the transparency range of the crystal.

LBO has recently received much attention in the frequency doubling of high-power Nd:YAG and Nd:YLF lasers, where its high damage threshold and temperature-tuned noncritical phase matching have challenged the dominance of KTP.[34,35] LBO has a transmission range

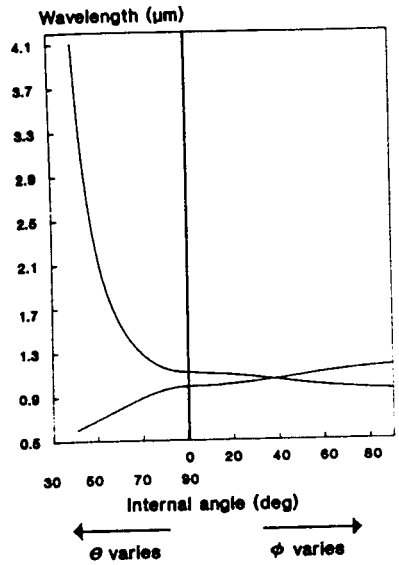

Fig. 1. Calculated tuning curves for KTP with a pump wavelength of 523 nm based on the Sellmeier relations of Bierlein and Vanherzeele.[32] Starting from the right-hand side of the x axis at $\theta = 90°$, $\phi = 90°$, which corresponds to propagation along the KTP crystallographic y axis, decreasing ϕ corresponds to angle tuning in the xy plane to $\phi = 0°$, which corresponds to propagation along the crystallographic x axis. Angle tuning is then away from the x axis in the zx plane, maintaining $\phi = 0°$ while θ varies.

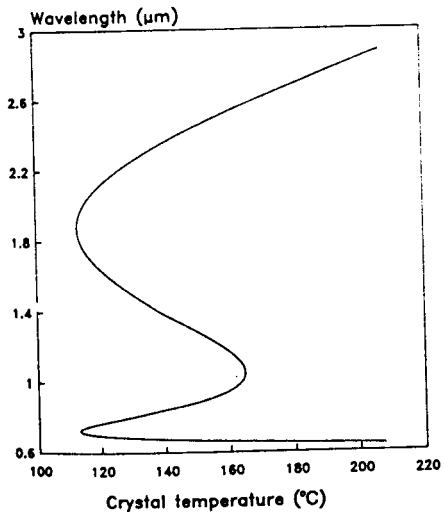

Fig. 2. Calculated temperature-tuning behavior for LBO with a pump wavelength of 523 nm based on the temperature-dependent Sellmeier relations of Lin *et al.*[37]

from 160 to 3000 nm. LBO's transmission to shorter wavelengths results in a low material dispersion across the visible and near-IR regions of the electromagnetic spectrum. Consequently LBO has a very large spectral-acceptance bandwidth and very low group-velocity dispersion in this spectral region. Thus, for a given pump-pulse duration, a much longer crystal length can be used with LBO than with KTP. The calculated bandwidth acceptance for a 12-mm-long crystal of LBO is 2.8 nm at a 1047-nm wavelength, and the group-velocity mismatch between pulses at the wavelengths 523 and 1047 nm is 0.05 ps mm^{-1}. One calculates by using the dispersion relations of Kato[36] that the external acceptance angles for temperature-tuned phase matching along the x axis are 64 mrad (xy) and 50 mrad (zx). The effective nonlinear coefficient d_{eff} is 1.2 pm V^{-1}, and the parametric gain corresponding to the same pump-beam parameters quoted above for KTP is $\eta(\Delta\nu_p)\eta(\Delta\theta_p)\Gamma'^2 l'^2 = 3.5 \times 10^{-3}$ MW^{-1} $cm^2 = 3.5$ W^{-1}. Thus one calculates from Eq. (9) that the threshold average power for a 3% round-trip cavity loss is 10 mW, which compares favorably with the calculation for KTP.

Because of the large temperature dependence of the birefringence of LBO, one can achieve temperature-tuned noncritical phase matching along the x axis. For a pump wavelength of 523 nm, one calculates, by using the temperature-dependent dispersion relations of Lin *et al.*,[37] a tuning range of 0.64–2.9 μm for a temperature variation of 100 °C that is due to the phase-matching retracing behavior, as shown in Fig. 2. This range is much larger than the tuning range for KTP in the xy plane and covers much of the region of interest in the near IR.

4. EXPERIMENTAL ARRANGEMENT AND CHARACTERIZATION OF THE SPOPO PERFORMANCE

A schematic of the experimental arrangement that we used is shown in Fig. 3. The pump laser was a self-starting additive-pulse mode-locked Nd:YLF laser pumped by a 3-W laser diode (SDL 2482 P1). The particulars of this laser have been previously described (Ref. 17; see also Ref. 38) and will only be summarized here. With a 3-W laser-diode pump source, 400–500 mW of average power could be achieved as usable output from the mode-locked Nd:YLF laser at 1047 nm in pulses of 2.0–2.4-ps duration of pulse-repetition rates of typically 125 MHz. We frequency doubled the mode-locked laser in a resonant external enhancement cavity by using temperature-tuned noncritically phase-matched MgO:$LiNbO_3$ as the nonlinear crystal. We routinely obtained an average output power of 250–270 mW from the enhancement cavity in pulses of 2-ps duration. This frequency-doubled output was in a diffraction-limited TEM_{00} beam.

We chose a ring cavity for the OPO rather than a linear standing-wave cavity. In this configuration the passive insertion loss of the nonlinear crystal is experienced only on a single pass per round trip of the resonator. In a standing-wave resonator, however, the crystal insertion loss is experienced twice per round trip, whereas the

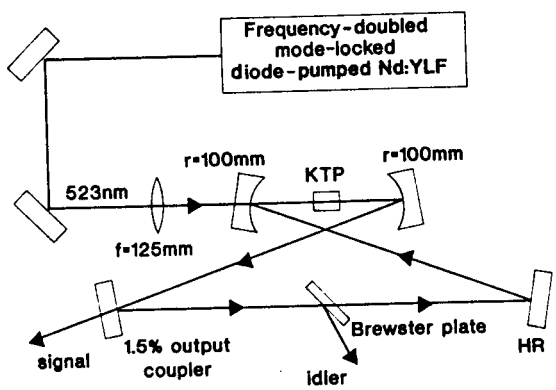

Fig. 3. Schematic of the experimental arrangement. HR, high reflector.

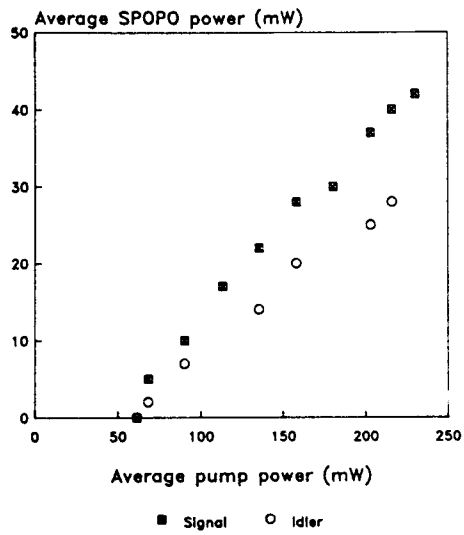

Fig. 4. Variation of the average signal and idler output power with the average pump power incident upon the KTP crystal.

gain, being demonstrated only when the signal and the idler are copropagating with the pump, is the same per round trip as in the ring configuration.

The orthogonally polarized generated waves can be resonated equally well. For convenience, we resonated the generated wave that is polarized parallel to the pump wave. An uncoated silica flat was oriented at the Brewster angle to transmit horizontally polarized light, as shown in Fig. 3. The Brewster plate also served to couple out ~34% of the nonresonated wave. This rejection of the idler wave might also be thought to contribute to the enforcement of singly resonant operation, although in fact we achieved singly resonant oscillation without recourse to active discrimination, as will be described below. The ring cavity consisted of two plane mirrors and two concave mirrors of 100-mm radius of curvature. Three of the mirrors were coated to be highly reflective (R = 99.7%) at the signal and idler wavelengths and highly transmissive (T = 90%) at the pump wavelength of 532 nm. The fourth mirror was a 1.5% transmitting output coupler for the resonated wave. The 100-mm radius-of-curvature mirrors permitted achievement of a resonated beam-waist size of 15–20 μm ($1/e^2$ intensity radius) over much of the stability range of the resonator. We kept the angle of incidence on the curved mirrors to ~2.5° to minimize astigmatism in the cavity.

The gain medium was a KTP crystal that was cut for quasi-noncritical type-II phase matching in the xy plane for frequency doubling between 1064 and 532 nm (θ = 90°, ϕ = 26°). The crystal dimensions were 5 mm × 5 mm × 5 mm, and the crystal was antireflection coated at 1064 and 532 nm on both faces. We deduced the crystal's insertion loss by measuring the OPO-cavity finesse. This indicated a total cavity loss of 3.1% per round trip, of which 1.0% was known to be contributed by the three highly reflective mirrors and 1.5% by the output coupler, implying that 0.6% was the single-pass loss of the crystal. We also obtained confirmation of these figures by relating the SPOPO external conversion efficiency to the degree of pump depletion to deduce the relative amounts of useful (output) loss to total cavity loss. We placed the KTP crystal at the intracavity waist between the two curved mirrors. With a 125-mm focal-length lens, the pump beam was focused down to a waist size of 16 μm at the site of the KTP crystal.

With the OPO cavity aligned and the length matched to the pump laser, we achieved optical parametric oscillation in a unidirectional beam that was copropagating with the pump beam, with the resonated signal pulse being pumped once per round trip by consecutive pump pulses. The result was a stable and continuous train of picosecond pulses in both the signal and the idler beams.

A typical plot of the variation of the signal and idler average power with average pump power measured near degeneracy is shown in Fig. 4. The oscillation threshold corresponded to 61 mW of average pump power at 523 nm incident upon the KTP crystal. This represented a pump-pulse peak power of ~230 W and a peak axis-power density of ~57 MW cm^{-2}. Given the various approximations made in the gain calculation of Section 3 above, the calculated threshold of 50 mW is in satisfactory agreement with the experimentally determined value. The SPOPO yielded an output-signal slope efficiency of 21% with respect to power incident upon the SPOPO cavity, giving rise to an average signal-output power of 42 mW at the maximum available pump power of 255 mW incident upon the OPO cavity. This represents an external conversion efficiency of 16% of the 523-nm pump into tunable signal output. In addition, 27-mW average power of the nonresonated idler wave was obtained owing to the reflection loss from the Brewster plate.

The Brewster plate was originally incorporated to contribute toward discrimination against one of the generated waves so as to enforce singly resonant operation. In fact, singly resonant operation occurred equally well without the Brewster plate, since it was impossible to satisfy the synchronism requirements for both waves simultaneously. Thus the requirements for synchronism between the SPOPO and the pump laser resulted in a maximum length detuning of ~40 μm for either polarization with respect to exact length matching before oscillation ceased, whereas the two cavity-length settings for synchronism of the orthogonally polarized waves differed by ~3 mm because of the birefringence of KTP.

The pump depletion (total conversion efficiency) and the signal efficiency (average signal output to average pump incident upon the crystal) are shown in Fig. 5. These

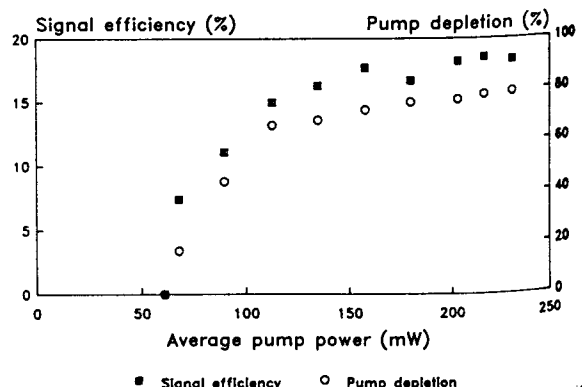

Fig. 5. Variation of the pump depletion and signal efficiency (ratio of average signal-output power to average pump power incident upon the KTP crystal) with average pump power incident upon the KTP crystal.

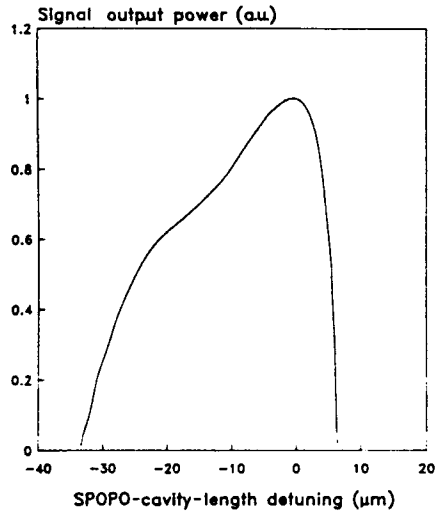

ig. 6. Variation of the average signal-output power with POPO-cavity-length detuning at a pump power of 200 mW at 3 nm incident upon the SPOPO cavity.

urves show that the efficiency starts to roll over at ~2 mes threshold. The Cheung–Liu[21] simulations indicate at the efficiency peaks at 3–4 times threshold at optium length detuning and then decreases with increased ump power beyond this level. However, the signal intenity monotonically increases with increasing pump power.

We analyzed the output beam of the resonated wave rom the SPOPO with a commercial beam profiler (Big Sky eam analyzer). The output beam was TEM_{00}, with a eam-waist size of 600 μm in the collimated arm of the POPO cavity. We measured the corresponding far-field ivergence to be 0.6 mrad. Thus the signal beam was early diffraction limited, and small focal spot sizes hould be possible.

The signal efficiency (output power) versus the SPOPOavity-length detuning is shown in Fig. 6. The form of hese curves is similar to those of Piskarskas[6] and to the heung–Liu[21] simulations. The signal efficiency curve is ot symmetric near zero cavity-length detuning. Cheung nd Liu[21] suggested that such an asymmetry is due to the nterplay of intensity-dependent and detuning-dependent hase-shift terms in the expression for the gain of the POPO.

The efficiency of the SRO has been considered by a umber of authors. In the plane-wave limit the cw SRO eaches 100% efficiency at ~2.5 times threshold.[26] Pumping beyond this level results in a power transfer ack to the pump from the signal and idler. By considerng the transverse spatial variation of a Gaussian pump eam, Bjorkholm[39] showed that the SRO reaches a maxium efficiency of ~70% at 6.5 times threshold. In their umerical simulations Cheung and Liu[22] considered a cw POPO operating near 2 μm pumped by a TEM_{00} Gaussan beam at 1053 nm. They found that for a 30-ps pump ource a maximum efficiency of ~60% was achieved at 2 imes threshold, whereas for a 5-ps pump source the maxium efficiency was 70% at 2.8 times threshold. Our reults cannot be directly compared with the Cheung–Liu alculations, but with 80% conversion efficiency at 3.7 mes threshold our results confirm that high efficiency an be achieved in practice.

The variation of the signal-pulse duration (FWHM) with average pump power at optimum length detuning is shown in Fig. 7. The form of the variation agrees with the analysis of Becker *et al.*[25] and with the Cheung–Liu[21] simulations. Near threshold, depletion of the pump beam is negligible. Because there is no gain storage in the parametric interaction the signal-pulse duration is determined by that part of the pump pulse that is above threshold. In the absence of other effects, e.g., pulse walk-off, significant pulse shortening of the signal pulse relative to the pump pulse can then result. The signal-pulse duration near threshold is determined by the interplay of signal-pulse shortening that is due to the negative curvature of the pump pulse and the small but significant dispersive pulse broadening that is due to the intracavity elements. The results of Becker *et al.*[25] indicate a minimum achievable pulse duration of ~0.4 times the pump-pulse duration. As the signal intensity grows with increasing pump power, depletion of the pump pulse will preferentially occur at the peak of the pulse, reducing the negative curvature of the pump-pulse envelope. Under strong pump depletion the curvature of the pump pulse can eventually change sign toward the end of the crystal. This can cause the signal and idler pulses to broaden in this region, beyond the initial pump-pulse width, to as much as ~1.5 times the pump-pulse duration.[25] These predicted minimum and maximum signal-pulse durations take no account of the broadening effects of temporal pulse walk-off.

We found that the spectrum of the SPOPO output had a smooth profile and a stable center frequency, as measured with a grating optical spectrum analyzer with a resolution of 0.1 nm. At a pump power of 200 mW incident upon the SPOPO cavity the FWHM signal spectrum was 0.77 nm at 1047 nm. The corresponding signal-pulse width was 1.5 ps as measured by background-free intensity autocorrelation, giving a time–bandwidth product of 0.32. In fact, throughout the operating range of the SPOPO the time–bandwidth product was in the range of 0.32–0.34, near that for transform-limited $sech^2$ pulses. The transform-limited nature of the SPOPO pulses was confirmed by interferometric autocorrelations, with a typical

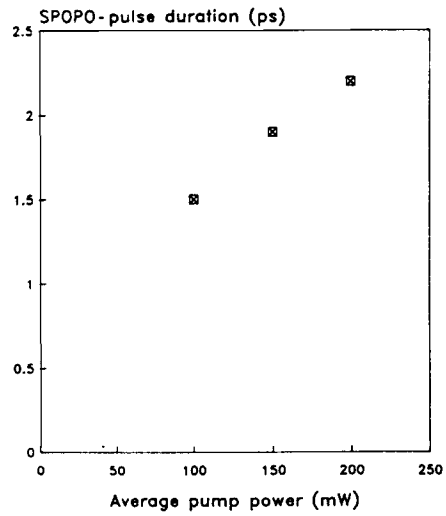

Fig. 7. Variation of the signal-pulse duration FWHM with average pump power at 523 nm incident upon the KTP crystal.

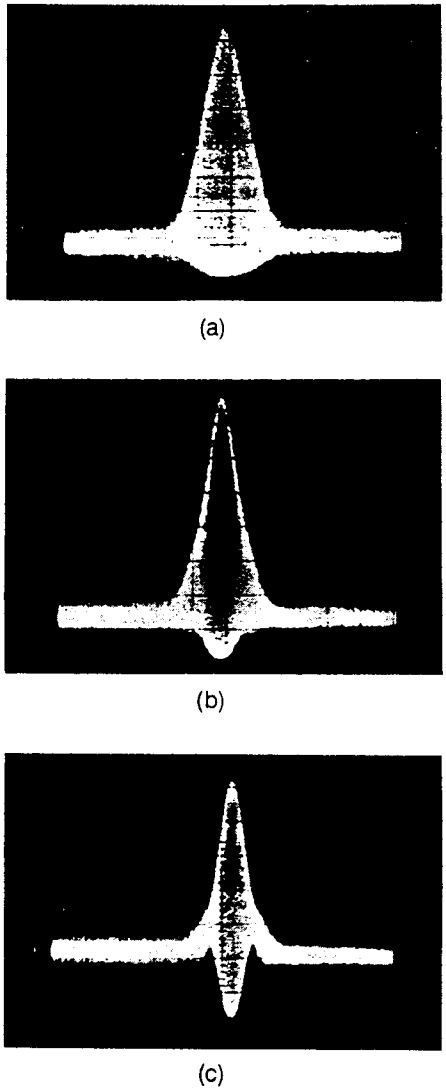

Fig. 8. Interferometric autocorrelations of the signal-output pulse. (a) At optimum length detuning, the signal pulse is transform limited, as indicated by the interference fringes extending out into the wings of the autocorrelation. With increasing SPOPO-cavity detuning to longer cavity lengths the signal pulses progressively shorten and acquire an increasing chirp, as indicated by the rising wings of the autocorrelation in (b) ~4-μm detuning and (c) ~8-μm detuning.

result shown in Fig. 8(a). The interference extending out into the wings of the autocorrelation indicates an absence of substructure in the pulse.

We also observed that the variation of the signal-pulse duration with cavity-length detuning was in qualitative agreement with the Cheung–Liu[21] simulations. Detuning to shorter SPOPO-cavity lengths resulted in a gradual broadening and a decrease in intensity of the signal pulses. Interferometric autocorrelations indicated that the pulses remained essentially transform limited. By contrast, detuning to longer SPOPO-cavity lengths resulted in a sharp reduction in the signal-pulse duration. At 200 mW pump power, lengthening the SPOPO cavity by ~8 μm from optimum length mismatch reduced the signal-pulse duration from 1.5 to 0.95 ps and increased the bandwidth from 0.76 to 1.24 nm. Interferometric autocorrelations indicated that these pulses were increasingly chirped with increasing cavity-length detuning, as indicated by the rising wings of the autocorrelations in Figs. 8(b) and 8(c).

Tuning of the SPOPO was accomplished by rotation of the crystal about its z axis, i.e., changing the direction of propagation in the xy plane. Since rotation of the crystal resulted in misalignment of the SPOPO cavity, we accomplished tuning by making sequential adjustments in the crystal angle, cavity alignment, and cavity length. The calculated tuning curve for KTP in the xy and zx principal planes is shown in Fig. 1 above. We observed that the experimentally measured tuning behavior closely followed the predicted tuning behavior. In the xy plane the resonated wave tuned from 1039–1096 nm and the unresonated wave tuned from 1056 to 1002 nm for a crystal rotation of 26° (internal angle). We obtained the measured data by using a grating optical spectrum analyzer with a resolution of 0.1 nm. The slow tuning rate for the quasi-noncritically phase-matched interaction is evident from Fig. 1. The maximum attainable tuning range in this configuration is ~950–1150 nm for a 523-nm pump wavelength. This small tuning range is a necessary consequence of noncritical phase matching and is the principal drawback of this scheme. The tuning range of the SPOPO as reported in Ref. 17 was limited by the reflectivity range of the mirrors used. We had not specified that any of the mirrors be broadband, with the operating range of the high reflectors being 960–1140 nm. However, the output coupler was operating at the edge of its reflectivity range, e.g., the output-coupler transmission had increased to 10% at 1005 nm. We then replaced the initial mirror set with a set from a commercial Ti:sapphire laser, which was highly reflective over the range of 950–1200 nm and highly transmissive at 523 nm, with the output coupler having 2% transmission over this range. We then extended the tuning range of the SPOPO by rotating the KTP crystal so that the propagation direction moved out of the xy plane toward the z axis. Then the resonated wavelength could be tuned from 1080 to 1184 nm and the nonresonated wavelength could be tuned from 938 to 1016 nm. Thus the SPOPO could be continuously tuned over the range of 938–1184 nm. The tuning range was then limited by the large angle of crystal rotation (35° external angle), reducing the effectiveness of the antireflection coatings and also causing clipping of the resonated beam.

As indicated above, since this SPOPO operated as a singly resonant device the operating wavelengths were stable, unlike the situation in typical DRO devices. Also, the signal- and idler-pulse intensities were not sensitive to fluctuations in pump intensity, as indicated in Fig. 5 above, particularly for operation at more than twice threshold. Operating at the optimum length provided stability against cavity-length fluctuations. Using an oscilloscope, we directly measured the amplitude noise on the SPOPO output to be 4% rms in the range of dc–5 kHz.

An additional stability mechanism previously observed by Edelstein *et al.*[7] is a shift in the center wavelength of the signal pulse with cavity-length detuning. The signal-pulse center wavelength shifts to a more favorable group velocity to compensate for the change in cavity-round-trip time. In this manner limited tuning of the SPOPO is possible because of group-velocity dispersion by tuning the cavity length of the SPOPO. For the present SPOPO we observed a small tuning of 0.2 nm in tuning the cavity

length over the total operating range of the SPOPO of 40 μm. This shift is much smaller than that observed by Edelstein *et al.* and reflects the relative insensitivity to group-velocity dispersion effects of pulses of ≥1-ps duration.

On occasions we observed that the average output power from the SPOPO slowly decayed over a period of ~10 min. Altering the alignment of the SPOPO cavity or the cavity length did not restore the output, nor did adjustments to the pump focusing optics. However, simple transverse translation of the KTP crystal did restore the output. The occurrence of this phenomenon appeared to be random in terms of the site pumped in the crystal because on many occasions the SPOPO operated without displaying this effect. Examination of the crystal revealed no obvious defects. Indeed, the effect did not appear to be permanent, i.e., the SPOPO output was recovered if we blocked the pump beam for a sufficient length of time.

We attributed this decay to gray tracking (bulk darkening). This is a common phenomenon in KTP that is used for frequency doubling of high-power Nd:YAG lasers and can limit the conversion efficiency. Jacco *et al.*[40] made a quantitative analysis of this bulk-darkening phenomenon for flux-grown KTP. Their results showed that bulk-darkening severity increases with fluence and exposure time. Irreversible darkening occurred with prolonged exposure at an intensity of ~1 GW cm^{-2}. Operating below this level caused reversible bulk darkening in that the crystal could recover 100% transmission after ~1 day. They also found that operating the KTP crystal at elevated temperatures (100–200 °C) significantly improved KTP's resistance to the onset of bulk darkening and hastened the recovery from bulk darkening compared with room temperature. Finally, Jacco *et al.* found that bulk darkening required the presence of visible ($\lambda \sim 500$ nm) light.

The introduction of a simple heater to operate the KTP crystal at an elevated temperature could reduce the susceptibility of the crystal to bulk darkening. However, the additional complication may not be needed, since with our crystal we could always find a site where continuous operation of the SPOPO could be sustained without any sign of gray tracking at the maximum intensity levels available.

5. FUTURE DEVELOPMENTS

We have described the design and operation of a cw-pumped singly resonant SPOPO. The oscillation threshold pump intensity of 57 MW cm^{-2} (61-mW average power) was shown to be in reasonable agreement with approximate calculations. With an all-solid-state pump source providing 2-ps pulses at 523 nm, the SPOPO provided transform-limited pulses of 1–2-ps duration that were continuously tunable over the range of 938–1184 nm, with tens of milliwatts of average power and peak powers of as much as ~200 W.

The limited tuning range of this KTP SPOPO is a consequence of our having to operate with an angle-tuning scheme with quasi-noncritical phase matching, which was required to minimize the oscillation threshold pump power. The potential tuning range for a 523-nm pumped KTP SPOPO as permitted by phase matching and optical transmission is 590–4500 nm. However, a crystal with a suitable orientation for widely tunable operation would involve a large Poynting-vector walk-off (up to ~50 mrad) and would necessitate a multiwatt average power picosecond source at 523 nm for efficient operation over this range. This could conceivably be achieved in a number of ways, one of which could be to amplify the output of our existing mode-locked laser before second-harmonic generation.

LBO appears to be a more promising candidate for widely tunable operation with modest (i.e., <1-W) pump power. Typical calculated gains for LBO under noncritical phase matching are higher than are those for KTP. This is due to the longer crystal lengths that can be exploited, with LBO more than offsetting the reduced nonlinear coefficient compared with KTP. In addition, one can maintain this high gain over the entire tuning range because of the large temperature dependence of the birefringence in LBO. The potential temperature-tuning range for a 523-nm-pumped SPOPO in LBO is ~630–3000 nm. The major complication with the substitution of LBO as the gain medium is the requirement for uniform heating of the crystal to vary its temperature over the range ~100–200 °C without temperature gradients along its length or over its cross section. In addition, LBO has a large anisotropic thermal expansion, and in the past this has caused problems with the durability of antireflection coatings that must withstand temperature cycling. It is possible that a Brewster-angled crystal would provide an effective alternative to antireflection coatings by negating the need for the latter altogether. In addition, this configuration would avoid the problem of spectral roll-off that is associated with antireflection coatings, thus providing a low reflection loss across the entire tuning range.

ACKNOWLEDGMENTS

This research was supported in part by the UK Science and Engineering Research Council, whose support in the form of a research studentship is also acknowledged by M. J. McCarthy. The assistance of S. Butterworth in obtaining the interferometric autocorrelations is also appreciated.

REFERENCES

1. J. A. Giordmaine and R. C. Miller, "Tunable coherent parametric oscillation in $LiNbO_3$ at optical frequencies," Phys. Rev. Lett. **14**, 973–976 (1965).
2. T. Kushida, Y. Tanaka, and M. Ojima, "Tunable picosecond pulse generation by optical parametric oscillation," Jpn. J. Appl. Phys. **16**, 2227–2235 (1977).
3. L. J. Bromley, A. Guy, and D. C. Hanna, "Synchronously pumped optical parametric oscillation in beta-barium borate," Opt. Commun. **67**, 316–320 (1988).
4. L. J. Bromley, A. Guy, and D. C. Hanna, "Synchronously pumped optical parametric oscillation in KTP," Opt. Commun. **70**, 350–354 (1989).
5. A. Piskarskas, V. Smilgevicius, and A. Umbrass, "The parametric generation of bandwidth limited picosecond light pulses," Opt. Commun. **73**, 322–324 (1989).
6. A. Piskarskas, V. Smilgevicius, and A. Umbrass, "Continuous parametric generation of picosecond light pulses," Sov. J. Quantum Electron. **18**, 155–156 (1988).
7. D. C. Edelstein, E. S. Wachman, and C. L. Tang, "Broadly tunable high repetition rate femtosecond optical parametric oscillator," Appl. Phys. Lett. **54**, 1728–1730 (1989).

8. E. S. Wachman, D. C. Edelstein, and C. L. Tang, "Continuous-wave mode-locked and dispersion-compensated femtosecond optical parametric oscillator," Opt. Lett. **15**, 136–138 (1990).
9. E. S. Wachman, W. S. Pelouch, and C. L. Tang, "Cw femtosecond pulses tunable in the near- and midinfrared," Z. Appl. Phys. **70**, 1893–1895 (1991).
10. G. Mak, Q. Fu, and H. M. van Driel, "Externally pumped high repetition rate femtosecond infrared optical parametric oscillator," Appl. Phys. Lett. **60**, 542–544 (1992).
11. W. S. Pelouch, P. E. Powers, and C. L. Tang, "Ti:sapphire-pumped, high-repetition-rate femtosecond optical parametric oscillator," Opt. Lett. **17**, 1070–1072 (1992).
12. Q. Fu, G. Mak, and H. M. van Driel, "High-power, 62-fs infrared optical parametric oscillator synchronously pumped by a 76-MHz Ti:sapphire laser," Opt. Lett. **17**, 1006–1008 (1992).
13. G. T. Maker and A. I. Ferguson, "Doubly resonant optical parametric oscillator synchronously pumped by a frequency doubled mode-locked and Q-switched diode laser pumped neodymium yttrium lithium fluoride laser," Appl. Phys. Lett. **56**, 1614–1616 (1990).
14. M. Ebrahimzadeh, G. J. Hall, and A. I. Ferguson, "Picosecond infrared optical parametric generation in KTP using a diode-laser-pumped solid-state laser," Opt. Lett. **16**, 1744–1746 (1991).
15. M. Ebrahimzadeh, G. J. Hall, and A. I. Ferguson, "Singly resonant, all-solid-state, mode-locked LiB_3O_5 optical parametric oscillator tunable from 652 nm to 2.65 μm," Opt. Lett. **17**, 652–654 (1992).
16. M. Ebrahimzadeh, G. P. A. Malcolm, and A. I. Ferguson, "Continuous-wave mode-locked optical parametric oscillator synchronously pumped by a diode-laser-pumped solid-state laser," Opt. Lett. **17**, 183–185 (1992).
17. M. J. McCarthy and D. C. Hanna, "Continuous-wave mode-locked singly resonant optical parametric oscillator synchronously pumped by a laser-diode-pumped Nd:YLF laser," Opt. Lett. **17**, 402–404 (1992).
18. A. Robertson, G. P. A. Malcolm, M. Ebrahimzadeh, and A. I. Ferguson, "Continuous generation of tunable picosecond pulses from 650 nm to 2.7 μm using a cw, synchronously pumped, all-solid-state, four-color LiB_3O_5 optical parametric oscillator," in *Conference on Lasers and Electro-Optics*, Vol. 12 of 1992 OSA Technical Digest Series (Optical Society of America, Washington, D.C., 1992), pp. 663–664.
19. G. D. Boyd and D. A. Kleinman, "Parametric interaction of focused Gaussian light beams," J. Appl. Phys. **19**, 3597–3639 (1968).
20. S. Guha and J. Falk, "The effects of focusing on parametric oscillation," IEEE J. Quantum Electron. **QE-18**, 907–912 (1982).
21. E. C. Cheung and J. M. Liu, "Theory of a synchronously pumped optical parametric oscillator in steady state," J. Opt. Soc. Am. B **7**, 1385–1401 (1990).
22. E. C. Cheung and J. M. Liu, "Efficient generation of ultrashort wavelength tunable infrared pulses," J. Opt. Soc. Am. B **8**, 1491–1506 (1991).
23. S. J. Brosnan and R. L. Byer, "Optical parametric oscillator threshold and linewidth studies," IEEE J. Quantum Electron. **QE-15**, 415–431 (1979).
24. D. C. Edelstein, "New sources and techniques for ultrafast laser spectroscopy," Ph.D. dissertation (Cornell University, Ithaca, N.Y., 1990).
25. M. F. Becker, D. J. Kuizenga, D. W. Phillion, and A. Siegman, "Analytical expressions for ultrashort pulse generation on mode-locked optical parametric oscillators," J. Appl. Phys. **45**, 3996–4005 (1974).
26. R. L. Byer, "Parametric oscillators and nonlinear materials," in *Nonlinear Optics*, P. G. Harper and B. S. Wherrett, eds. (Academic, San Francisco, Calif., 1977), pp. 47–160.
27. S. A. Akhmanov, A. S. Chirkin, K. N. Drabovich, A. I. Kovrigin, R. V. Khokhlov, and A. P. Sohorukov, "Nonstationary nonlinear optical effects and ultrashort light pulse formation," IEEE J. Quantum Electron. **QE-4**, 598–605 (1968).
28. H. Kogelnik, "Coupling and conversion coefficients for optical modes,"in *Proceedings of the Symposium on Quasi-Optics* (Polytechnic, New York, 1964), Vol. 14, pp. 333–347.
29. M. A. Persaud, J. M. Tolchard, and A. I. Ferguson, "Efficient generation of picosecond pulses at 243 nm," IEEE J. Quantum Electron. **26**, 1253–1258 (1990).
30. D. Hon, "High average power efficient second harmonic generation," in *Laser Handbook*, M. L. Stitch, ed. (North Holland, Amsterdam, 1979), pp. 421–484.
31. T. Y. Fan, C. E. Huang, B. Q. Hu, R. C. Eckardt, Y. X. Fan, R. L. Byer, and R. S. Feigelson, "Second harmonic generation and accurate index of refraction measurements in flux grown $KTiOPO_4$," Appl. Opt. **26**, 2390–2394 (1987).
32. J. Bierlein and H. Vanherzeele, "Potassium titanyl phosphate: properties and new applications," J. Opt. Soc. Am. B **6**, 622–633 (1989).
33. R. C. Eckardt, H. Masuda, Y. X. Fan, and R. L. Byer, "Absolute and relative nonlinear optical coefficients of KDP, KD*P, BaB_2O_4, $LiIO_3$, MgO:$LiNbO_3$, and KTP measured by phase matched second harmonic generation," IEEE J. Quantum Electron. **26**, 922–933 (1990).
34. J. Y. Huang, Y. R. Shen, C. Chen, and B. Wu, "Noncritically phase-matched second harmonic generation and optical parametric amplification in a lithium triborate crystal," Appl. Phys. Lett. **58**, 1579–1581 (1991).
35. S. T. Yang, C. C. Pohalski, E. K. Gustafson, R. L. Byer, R. S. Feigelson, R. J. Raymakers, and R. K. Route, "6.5-W, 532-nm radiation by cw resonant external-cavity second-harmonic generation of an 18-W Nd:YAG laser in LiB_3O_5," Opt. Lett. **16**, 1493–1495 (1991).
36. K. Kato, "Tunable uv generation to 0.2325 μm in LiB_3O_5," IEEE J. Quantum Electron. **26**, 1173–1175 (1990).
37. S. Lin, J. Y. Huang, J. Ling, C. Chen, and Y. R. Shen, "Optical parametric amplification in a lithium triborate crystal tunable from 0.65 to 2.5 μm," Appl. Phys. Lett. **59**, 2805–2807 (1991).
38. M. J. McCarthy, G. T. Maker, and D. C. Hanna, "Efficient frequency doubling of a self-starting additive-pulse mode-locked diode pumped Nd:YAG laser," Opt. Commun. **82**, 327–332 (1991).
39. J. E. Bjorkholm, "Some effects of spatially nonuniform pumping in pulsed optical parametric oscillators," IEEE J. Quantum Electron. **QE-7**, 109–118 (1971).
40. J. Jacco, D. R. Rockafellow, and E. A. Teppo, "Bulk-darkening threshold of flux-grown $KTiOPO_4$," Opt. Lett. **16**, 1307–1309 (1991).